1

A NEAR-INFRARED SPECTROSCOPIC DATABASE OF HIGH-REDSHIFT QUASARS

1.1 INTRODUCTION

With the exception of a handful of very nearby objects, the inner regions of AGNs cannot be resolved. Spectroscopy is therefore an invaluable tool in virtually all AGN-related science. The optical region of a quasar spectrum includes a number of strong emission features, including the broad Balmer lines Hα (6565 Å) and Hβ (4863 Å) and the narrow [O III]$\lambda\lambda$4960,5008 doublet. These emission lines are a rich source of information on fundamental properties of AGNs and quasars. As we will see in Chapter **??**, the Balmer lines are routinely used to derive BH masses and AGN accretion rates. As the strongest narrow emission line in the optical spectrum, [O III] is used to measure systemic redshifts, and to probe AGN-driven outflows in the NLR (see Chapter **??**).

Large optical surveys have provided spectra for hundreds of thousands of AGN and quasars. With it's twelfth data release in 2016, the number of AGNs and quasars in the Sloan Digital Sky Survey (SDSS; York et al., 2000) spectroscopic catalogue alone reached almost $300,000$. However, the rest-frame optical region is redshifted beyond the reach of optical spectrographs at redshifts $z \gtrsim 0.4$. Accessing the rest-frame optical lines at redshifts $2 \lesssim z \lesssim 4$, during the peak epoch of galaxy evolution, requires near-infrared spectroscopy.

Spectroscopic observations are more challenging at near-infrared wavelengths than in the optical because the Earth's atmosphere is both bright and highly variable at infrared wavelengths. As a result, the number of high-redshift quasars with near-infrared spectra is limited and previous investigations of the rest-frame optical spectra of quasars at redshifts $z \sim 2$ have typically used samples containing a few dozen objects (e.g. Marziani et al., 2009; Shen and Liu, 2012; Shen, 2016).

In this Chapter, I will describe the construction of a database containing 434 high-redshift quasars. In later Chapters, I will describe how I have used this data to significantly reduce large systematic biases afflicting BH mass estimates for quasars at

Table 1.1: Summary of near-infrared spectroscopic database.

Instrument	Number
FIRE/Magellan	36
GNIRS/Gemini	29
ISAAC/VLT	13
LIRIS/WHT	21
NIRI/Gemini	31
NIRSPEC/Keck	3
SINFONI/VLT	84
SofI/NTT	111
TRIPLESPEC/ARC	38
TRIPLESPEC/Hale	60
XSHOOTER/VLT	36
Total	462

redshifts $z \gtrsim 2$ (Chapter **??**) and to study the prevalence and drivers of quasar-driven galaxy-wide outflows (Chapter **??**). The unprecedented size and quality of this dataset make a number of other interesting investigations possible, some of which are described in Chapter **??**.

1.2 DATA

The near-infrared spectra in our database are taken from published catalogues, by downloading and reducing archival spectra, and by reducing previously un-published spectra acquired in programmes led by Prof. J. Hennawi (UCSB) and Prof. X. Prochaska (UCO/LICK). As the P.I. of two programmes, I targeted quasars with the goal of filling in under-sampled regions of the C IV EQW and blueshift parameter space (see Section XX for a detailed discussion of C IV emission properties in high-redshift quasars). The telescopes and instruments used to observe the spectra are summarised in Table 1.1 and information on individual spectra is provided in Table 1.2. There are 434 unique quasars in our catalogue. Multiple spectra exists for a number of quasars, and so the total number of spectra in our catalogue is 462. The columns in Table 1.2 are as follows:

1 ID: Jhhmmss+ddmmss. ID is repeated when multiple spectra exist for the same object.

2 Unique catalogue name.

3 Date spectrum acquired.

4-5 RA and DEC (J2000; truncated coordinates).

6 Instrument and telescope used to acquire spectrum.

7 Wavelength range covered by spectrum.

8 Velocity per pixel in spectrum.

9 S/N per pixel in spectrum.

10 Redshift.

Table 1.2: Quasars in our near-infrared spectroscopic database. Only the first 15 entries are shown. The full table (including 462 objects) is available online.

ID	Cat. Name	Date	Ra	Dec	Instr.	$\Delta\lambda$ [μm]	Δv [km s^{-1}]	S/N	z
(1)	(2)	(3)	(4)	(5)	(6)	(7)	(8)	(9)	(10)
J000039-001804	QSO460	2015-09-02	+00h00m39.00s	-00d18m03.90s	SofI/NTT	1.50-2.54	154.0	4.9	2.14
J000345-232353	QSO552	2009-07-07	+00h03m45.00s	-23d23m53.40s	SINFONI/VLT	1.44-1.87	36.0	12.7	2.27
J000345-232353	QSO330	2011-09-18	+00h03m45.00s	-23d23m53.40s	SofI/NTT	1.48-1.83	63.0	36.0	2.26
J000451-084450	QSO290	2013-07-12	+00h04m50.66s	-08d44m49.63s	XSHOOTER/VLT	0.31-2.28	15.0	10.3	3.00
J000451-084452	QSO289	2013-08-08	+00h04m50.91s	-08d44m51.98s	XSHOOTER/VLT	0.31-2.28	15.0	5.4	3.00
J000500-003348	QSO454	2015-09-01	+00h05m00.42s	-00d33m48.20s	SofI/NTT	1.50-2.54	154.0	8.2	2.18
J000501+010221	QSO459	2015-09-02	+00h05m00.53s	+01d02m20.80s	SofI/NTT	1.50-2.54	154.0	6.8	2.13
J001016+001228	QSO475	2015-09-04	+00h10m16.49s	+00d12m27.60s	SofI/NTT	1.50-2.54	154.0	8.9	2.28
J001247+001239	QSO082	2013-06-06	+00h12m47.12s	+00d12m39.49s	ISAAC/VLT	1.52-1.60	15.0	19.1	2.16
J001708+813508	QSO107	2012-08-04	+00h17m08.48s	+81d35m08.10s	TRIPLESPEC/Hale	0.94-2.80	39.0	36.5	3.40
J001919+010152	QSO476	2015-09-04	+00h19m19.31s	+01d01m52.20s	SofI/NTT	1.50-2.54	154.0	6.5	2.32
J001955-091316	QSO001	2004-11-26	+00h19m54.67s	-09d13m16.45s	GNIRS/Gemini	0.60-2.61	88.0	9.9	2.12
J002018-233654	QSO553	2009-07-07	+00h20m18.41s	-23d36m53.80s	SINFONI/VLT	1.44-1.87	36.0	16.9	2.30
J002023-414639	QSO554	2009-07-08	+00h20m23.38s	-41d46m38.90s	SINFONI/VLT	1.09-1.41	35.0	33.4	1.57
J002111-242247	QSO555	2009-07-16	+00h21m10.90s	-24d22m47.20s	SINFONI/VLT	1.44-1.86	36.0	11.1	2.26

1.2.1 *Coatman et al., (2016) Quasars*

Target selection

We selected quasars from the Seventh Data Release (DR7; Schneider et al., 2010) of the SDSS spectroscopic quasar catalogue. The sample was restricted to objects with redshifts $2.14 < z < 2.51$ (7,258 quasars), to ensure that the Hβ and Hα emission lines fall within the H- and K-bands respectively, allowing us to observe both simultaneously with the appropriate grism configuration. Given the limited number of quasars for which near-infrared spectra could be obtained, the quasar sample was further restricted to objects that are radio-quiet (5,980 quasars), show no evidence of broad absorption lines (BALs) in their spectra (5,299 quasars), and are free from significant dust extinction. We removed radio-loud objects and BAL quasars using the classification flags described in Section 1.4.3. The removal of quasars with significant dust extinction was achieved by identifying quasars with $i - K$ colours redder than a parametric spectral energy distributions (SED) model combined with a SMC-like extinction curve with $E(B-V)$=0.05 (the SED model is described in Chapter **??**).

The K-magnitude (used to compute the $i - K$ colour) was taken from the UKIRT Infrared Deep Sky Survey (UKIDSS; Lawrence et al., 2007) Large Area Survey (ULAS). The requirement to be in the ULAS footprint and have reliable K band photometry reduced our sample of possible targets to 1,683, and the $E(B-V)$ cut left 1,204 in our sample. Finally, a flux-limit of $K < 18.5$ (AB) was applied to ensure that spectra of sufficient signal-to-noise ratio (S/N) could be obtained (leaving 412 quasars).

We were able to obtain new infrared spectra for 19 quasars from this sample of 412 possible targets. The quasars included in this sub-sample were selected to have C IV-emission shapes which span the full range observed in the population. Reliably quantifying the distribution of C IV-emission shapes has been made possible thanks to recent improvements in the estimation of systemic redshifts from ultraviolet spectra (see Section **??** for details).

Observations

Near-infrared spectra were obtained with the Long-slit Intermediate Resolution Infrared Spectrograph (LIRIS; Manchado

et al., 1998) mounted on the 4.2m William Herschel Telescope (WHT) at the Observatorio del Roque de los Muchachos (La Palma, Spain). Observations took place over four non-contiguous nights from 2015 March 31 to April 4. Approximately one night was lost due to poor weather and a further half-night was affected by poor transparency due to cloud. A one arcsecond slit-width was employed and the LIRIS $H+K$ low-resolution grism was selected, which covers the spectral ranges $1.53-1.79\,\mu m$ and $2.07-2.44\,\mu m$ with a dispersion of $9.7\,Å$/pixel. The spatial scale of the instrument is 0.25 arcsecond/pixel. Observations were divided into 60 second sub-exposures and performed in an ABBA nodding pattern, with the object placed at two positions along the slit 12 arcsecond apart. Bright $A0-5V$ stars were observed at similar air-masses to the targets in order to provide both telluric absorption corrections and a flux calibration of the quasar spectra.

Data reduction

The raw LIRIS data frames incorporate a known 'pixel shift' which was first removed from all frames using the LIRIS data reduction package `LIRISDR`. Subsequent data reduction was undertaken with standard `IRAF`[1] procedures[2]. The flat-field images, which were taken at the beginning of each night via illumination of the dome, were averaged and normalised to remove any wavelength-dependent signature. Each individual two-dimensional spectrum was then flat-field corrected. Consecutive AB and BA pairs of two-dimensional spectra were subtracted to remove the sky background. All the subtracted AB/BA-pairs for a given target were then averaged to give the final two-dimensional spectrum.

The size of the one-dimensional spectrum extraction windows, in the slit direction, varied from $6-10$ pixels. To increase the S/N, optimal variance-weighted extraction with sigma clipping was employed. For the fainter objects in our sample we were unable to trace the spectrum across the dispersion axis reliably and the trace from a telluric standard-star observation, observed at a similar air mass and time, was used instead. The

1 IRAF is distributed by the National Optical Astronomy Observatory, which is operated by the Association of Universities for Research in Astronomy (AURA) under a cooperative agreement with the National Science Foundation.

2 The data reduction pipeline is available at https://github.com/liamcoatman/SpectraTools

wavelength calibration, using argon and xenon lamp exposures, resulted in root mean square errors in the range $1.01 - 1.71$ Å, with a mean of 1.47 Å. The telluric standard star observations were reduced using the same steps described above. The stellar continuum was divided out of the standard star spectrum, which was then divided into the quasar spectrum to remove telluric absorption features. The spectral type and magnitude of the standard star were used to flux calibrate the quasar spectrum both in a relative and absolute sense.

1.2.2 *Shen and Liu, (2012) and Shen, (2016) Quasars*

Shen, (2016) and Shen and Liu, (2012) obtained near-infrared spectroscopy for a sample of 74 luminous, $1.5 < z < 3.5$ quasars selected from the SDSS DR7 quasar catalogue. Targets were required to possess good optical spectra covering the C IV line and have redshifts $z \sim 1.5$, 2.1, and 3.3 to ensure that the Hβ-[O III] region was covered in one of the near-infrared JHK bands. Thirty-eight of the quasars were observed with TripleSpec (Wilson et al., 2004) on the Astrophysics Research Consortium (ARC) 3.5 m telescope, and 36 with the Folded-port InfraRed Echellette (FIRE; Simcoe et al., 2010) on the 6.5 m Magellan-Baade telescope. The reduction of the spectra is described in Shen, (2016) and Shen and Liu, (2012).

1.2.3 *Quasar Pairs*

A large part of our catalogue was observed as part of an ongoing effort to identify quasar pairs at very close projected separations (Quasars Probing Quasars[3]; Hennawi et al., 2006a; Hennawi et al., 2010). The primary science driver of this work is to study the circum-galactic medium of the foreground quasars in absorption (Hennawi et al., 2006b). Very accurate systemic redshift measurements are a requirement and a large amount of resources have been devoted to obtaining near-infrared spectra which cover low-ionisation broad lines or features from the quasar NLR (Prochaska and Hennawi, 2009; Lau, Prochaska, and Hennawi, 2016; Hennawi et al., 2015).

Twenty-nine quasars were observed with the Gemini Near-Infrared Spectrograph (GNIRS; Elias et al., 2006) on the 8.1 m Gemini North telescope, thirteen using the Infrared Spectrome-

3 www.ucolick.org/~xavier/QPQ/Quasars_Probing_Quasars

ter And Array Camera (ISAAC; Moorwood et al., 1998) on the European Southern Observatory (ESO) Very Large Telescope (VLT), thirty-one with the Near InfraRed Imager and Spectrometer (NIRI; Hodapp et al., 2003) also on Gemini North and thirty-six with XSHOOTER (Vernet et al., 2011), again, on the VLT.

The XSHOOTER spectra were reduced with a custom software package developed by George Becker (for details, see Lau, Prochaska, and Hennawi, 2016). The remaining data was processed with algorithms in the LowRedux[4] package (see Prochaska and Hennawi, 2009).

1.2.4 *VLT SINFONI Quasars*

We performed a search of the ESO archive for high-redshift quasars observed with the SINFONI integral field spectrograph (Eisenhauer et al., 2003; Bonnet et al., 2004) at VLT/UT4. We found 79 quasars with redshifts $1.5 < z < 3.7$ which have H and/or K SINFONI spectroscopy, covering the Hβ and Hα lines respectively. Seventy-two of the quasars are from a large programme led by L. Wisotzki (programme 083.B-0456(A)) to study the mass function and Eddington ratios of active BHs drawn from the Hamburg-ESO survey (Wisotzki et al., 2000). A further seven SINFONI spectra are from a programme led by J. D. Kurk (programme 090.B-0674(B)) to obtain reliable BH mass estimates from Hα/Hβ for a sample of radio-loud/radio-quiet SDSS quasars.

I reduced the SINFONI spectra using the package EASYSINF[5]. The package, which is based on the ESO-SINFONI pipeline, is described in Williams et al., (2016).

1.2.5 *ESO NTT SOFI Quasars*

One quarter of the quasar catalogue derives from a large programme (programme 187.A-0645; PI: J. Hennawi) to combine near-infrared spectra from SOFI (Moorwood, Cuby, and Lidman, 1998) on the 3.6 m New Technology Telescope (NTT) with archival high-resolution optical spectra from the UV-Visual Echelle Spectrograph (UVES; Dekker et al., 2000) at VLT/UT2 and the High Resolution Echelle Spectrometer (HIRES; Vogt

4 www.ucolick.org/~xavier/LowRedux
5 www.mrao.cam.ac.uk/~rw480/easysinf

et al., 1994) at Keck to construct a legacy database of bright, high-redshift ($2 < z < 4$) quasars with both rest-frame optical spectra, covering the Hβ-[O III] complex, and high-resolution rest-frame ultraviolet spectra. The main science goal is to obtain precise systemic redshifts which are crucial for the study of absorption line systems. Observations were undertaken over 16 nights from September 2011 to March 2013. I reduced these spectra using a custom pipeline using algorithms in the LowRedux package.

Over five nights from 2015 August 31 to September 4 we obtained near-infrared SOFI spectra for a further 26 quasars (programme 095.B-0644(A); PI: L. Coatman). These quasars were selected from the SDSS DR7 quasar catalogue using criteria very similar to those described above for the WHT sample. In particular, we selected quasars with large C IV blueshifts to improve the statistics in this region of the C IV emission-line parameter space. The spectra were reduced using the same LowRedux pipeline described above.

1.2.6 *Hale TripleSpec Quasars*

A further 60 quasars in our catalogue are bright SDSS quasars which were observed with the TRIPLESPEC spectrograph (Herter et al., 2008) on the Palomar 200-inch Hale telescope (P200). The objects were observed with the same science goals as the SOFI NTT large programme. The spectra were reduced using a custom pipeline, again using algorithms in the LowRedux package.

1.3 Redshift and luminosity distribution of catalogue

In Fig. 1.1 we show the luminosities and redshifts of the quasar sample relative to the redshift-luminosity distribution for the Seventh Data Release (DR7; Schneider et al., 2010) of the SDSS spectroscopic quasar catalogue. Our sample spans a redshift range $1.5 < z < 4.0$ and a bolometric luminosity range $10^{45.5} - 10^{48}$ erg s^{-1}. Spectra were obtained within one or more of the JHK pass-bands and the gaps in our sample coverage at $z \sim 1.8$ and $z \sim 3$ are due to the presence of atmospheric absorption. Obtaining near-infrared spectra of adequate resolution and signal-to-noise ratio (S/N) of even moderately bright quasars remains resource intensive. As a consequence, at fixed

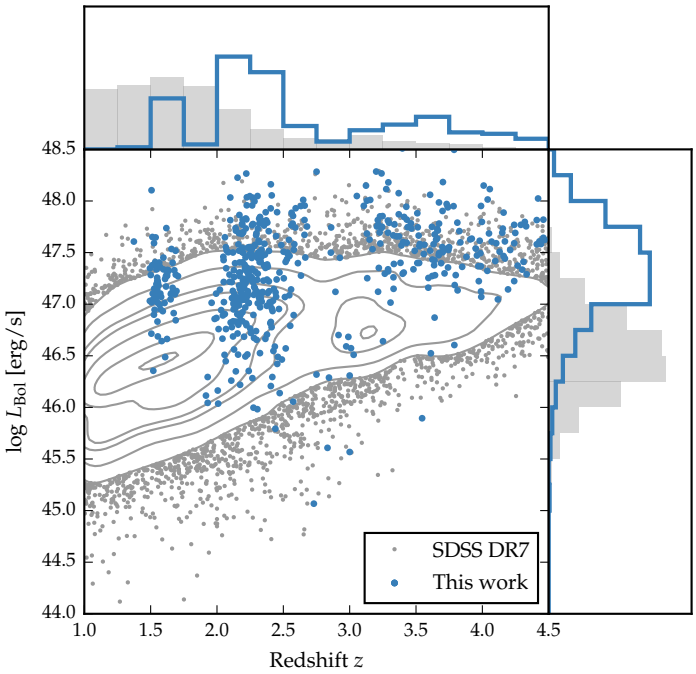

Figure 1.1: The ranges in redshift and luminosity covered by our sample, relative to the redshift-luminosity distribution of the SDSS DR7 quasar catalogue. In regions of high point-density, contours show equally-spaced lines of constant probability density generated using a Gaussian kernel-density estimator. For the SDSS sample we use Hewett and Wild, (2010) redshifts and bolometric luminosities measured by Shen et al., (2011). For the quasars in this work the redshift is defined using the peak of the Hα/Hβ emission and the luminosity is measured in the continuum at 1350Å and converted to a bolometric quantity using the same conversion factor employed by Shen et al., (2011).

redshift, the luminosities of the quasars are brighter than the average luminosity of the SDSS sample, although the dynamic range in luminosity is a full 1.5 decades.

1.4 SUPPLEMENTARY DATA

1.4.1 *Optical spectroscopic data*

Optical spectra are available for 79 per cent of the catalogue. The origin of these spectra is summarised in Table 1.3. The sources of the optical spectra employed are as follows:

Table 1.3: Percentage of catalogue for which optical spectroscopic data is available from the given sources.

	Source	%
(1)	SDSS	60
(2)	BOSS	45
(3)	HAMBURG-ESO	7
(4)	VLT/UVES	4
(5)	VLT/XSHOOTER	8

1. The Seventh Data Release (DR7; Schneider et al., 2010) of the SDSS spectroscopic quasar catalogue. Spectra are moderate resolution ($R \simeq 2000$) and S/N (S/N$\simeq$ 20) and cover the observed-frame wavelength interval $\sim 3800 - 9180$ Å.

2. The Twelfth Data Release (DR12; Pâris et al., 2017) of the Sloan Digital Sky Survey-III: Baryon Oscillation Spectroscopic Survey (SDSS-III/BOSS; Dawson et al., 2013). Compared to SDSS spectra, BOSS spectra cover a slightly broader wavelength range and are typically higher S/N.

3. The Hamburg-ESO survey (Wisotzki et al., 2000). The spectra have a typical $\sim 400\,\mathrm{km\,s^{-1}}$spectral resolution and S/N $\gtrsim$ 10 per pixel.

4. Spectra taken with VLT/UVES. The reduced and fluxed UVES spectra were made available to us by A. Dall'Aglio (a description of the reduction procedure is contained in Dall'Aglio, Wisotzki, and Worseck 2008). The spectral resolution of the UVES observations is very high ($R \sim 40,000$) and the S/N of the spectra, re-binned to a resolution of $\simeq 2000$, is S/N$\simeq$ 300.

5. Spectra taken with VLT/XSHOOTER. The XSHOOTER spectra are moderate resolution ($\sim$ 6000) and cover the full optical-near-infrared spectral region ($0.30 - 2.50\,\mu$m).

1.4.2 *Photometric data*

We cross-matched our catalogue with photometric data from the sources given below. The matching was done using a 5 arcsecond matching radius, with only the closest neighbour retained in the case of multiple matches. The cross-matched sur-

veys and the percentage of successful matches is summarised in Table 1.4. The columns in Table 1.4 are as follows:

1. SDSS DR9 photometric source catalogue. Point spread function magnitudes.
2. Two Micron All Sky Survey (2MASS; Skrutskie et al., 2006) Point Source Catalogue. Default magnitudes.
3. UKIRT Infrared Deep Sky Survey (UKIDSS; Lawrence et al., 2007) Large Area Survey (DR10). 1 arcsecond aperture corrected magnitudes ('apermag3').
4. Visible and Infrared Survey Telescope for Astronomy (VISTA) Hemisphere Survey (VHS; McMahon et al., 2013). 1 arcsecond aperture corrected magnitudes ('apermag3').
5. Kilo-Degree Infrared Galaxy (VIKING; Edge et al., 2013) Survey (DR4). 1 arcsecond aperture corrected magnitudes ('apermag3').
6. Wide-field Infrared Explorer (WISE; Wright et al., 2010) AllWISE Data Release (Mainzer et al., 2011). Profile-fitting magnitudes ('mpro').

1.4.3 *Radio/BALQSO classification*

Using the catalogues provided by Shen et al., (2011), Allen et al., (2011) and Pâris et al., (2017) and visual inspection, 19 quasars in the catalogue are identified as being C IV BALQSOs.

We cross-match our catalogue to the FIRST radio catalogue (White et al., 1997). We classify quasars with matches within 5 arcsecond as core-dominated, while, if multiple matches are found within 30 arcsecond, quasars are classified as lobe-dominated (e.g. Shen et al., 2011). 128 objects are outside of the FIRST footprint, 269 are not detected in FIRST, 29 are detected and are core-dominated, and 8 are detected and are lobe-dominated.

1.5 Absolute flux calibration of near-infrared spectra

Relative flux-calibration of the infrared spectra as a function of wavelength has been achieved through observations of appropriate flux standards. The absolute flux levels, however, can be

Table 1.4: Cross-matched surveys and the percentage of successful matches.

	SDSS	2MASS	UKIDSS	VHS	VIKING	WISE
	(1)	(2)	(3)	(4)	(5)	(6)
u	73	-	-	-	-	-
g	73	-	-	-	-	-
r	73	-	-	-	-	-
i	73	-		-	-	-
z	73	-	-	-	9	-
Y	-		41	10	9	-
J	-	57	41	34	9	-
H	-	57	41	20	9	-
K	-	57	41	33	9	-
*W*1	-	-	-	-	-	97
*W*2	-	-	-	-	-	97
*W*3	-	-	-	-	-	97
*W*4	-	-	-	-	-	97

in error by large factors due to variable atmospheric conditions combined with the narrow slit widths. For the majority of the quasars we have, therefore, established the absolute flux scale for each near-infrared spectrum using either the SDSS/BOSS spectroscopy or the available photometric data.

When a SDSS spectrum is available, we leverage the excellent flux calibration of these spectra to calibrate the near-infrared spectra. If a BOSS spectrum available, and an SDSS is not, then this is used instead. We use the quasar SED model described in Chapter **??** to bridge the gap between the wavelength coverage of the near-infrared and optical SDSS/BOSS spectra. The SED model, described in Chapter **??**, gives a very good fit to the SDSS and UKIDSS magnitudes of SDSS DR7 quasars, reproducing the individual magnitudes with a $\sigma < 0.1$ mag. The first step is to fit this quasar SED model to the SDSS/BOSS spectrum. The fit was done using a simple variance-weighted χ^2 minimisation procedure in several emission line-free intervals of the optical spectra. To avoid the known issues in the flux calibration of the BOSS DR12 quasar spectra at observed-frame blue wavelengths (Lee et al., 2013), our fitting was confined to rest-frame wavelengths long-ward of 1275 Å. The second step is to fit the near-infrared spectrum to the normalised SED model. Regions of the spectrum which fall between the near-infrared transmis-

Table 1.5: Methods used in absolute flux calibration of near-infrared spectra.

Method	%
SDSS	60
BOSS	9
NIR photometry	25
NIR+OPT photometry	6
None	1

sion bands are masked-out in the fitting procedure. The flux calibration method is demonstrated in Figure 1.2a.

If a SDSS/BOSS spectrum is unavailable, then a second flux calibration method is adopted. This method is identical, except that the SED model is first fit to the available optical (SDSS) and near-infrared (VHS, Viking, UKIDSS or 2MASS) photometric data. The SED model was integrated through the pass-band transmission functions, to give model magnitudes, and a variance weighted least-squares fit was done to the observed magnitudes. This is shown in Figure 1.2b.

We are unable to verify the absolute flux calibration of the near-infrared spectra for four objects because neither SDSS/-BOSS spectra nor optical/near-infrared data is available. The methods used to flux calibrate the near-infrared spectra are summarised in Table 1.5.

Ask Manda: (1+z) in luminosity calculation.

The flux at 1350 and 5100 Å was read off directly from the normalised SED model. These values were used to compute monochromatic continuum luminosities at 1350 and 5100 Å, which we use to estimate BH masses and bolometric luminosities in Chapters 3-5. Comparison of the 5100 Å luminosity, computed using the photometry- and spectrum-based methods for 296 quasars, showed a scatter (mean absolute deviation) of just $\sim$ 0.1 dex. We therefore assume 0.1 dex to be the measurement uncertainty on the 5100 Å luminosities. We expect the uncertainties on the 1350 Å luminosities to be at similar level. For all the catalogue quasars, the optical and near-infrared spectra as well as the near-infrared photometry were obtained at different epochs, with rest-frame time differences of up to $\sim$ 5 years. Intrinsic quasar photometric variability in the rest-frame ultraviolet and optical will therefore add additional scatter of $\sim$ 0.2 mag (e.g. MacLeod et al., 2010) to the derived 1350 and 5100 Åluminosities.

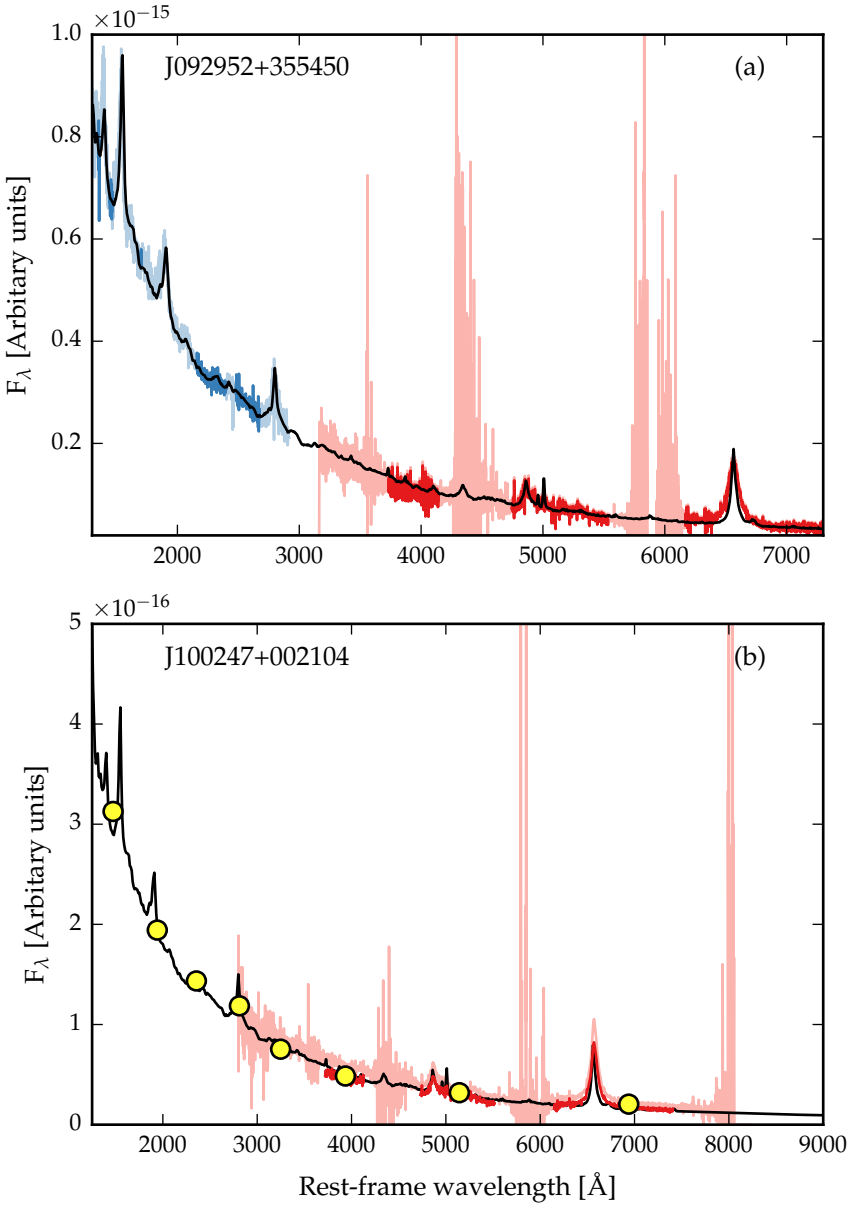

Figure 1.2: Demonstration of how the absolute flux calibration of the near-infrared spectrum (shown in red) is established using the SDSS spectrum (shown in blue, a) and photometric data (b). An empirical quasar SED model (shown in black) is used to bridge the discontinuity in the wavelength coverage of the optical/near-infrared spectroscopic and photometric data. The darker regions of the spectra are used in the fitting procedures.

Table 1.6: Measured spectral resolutions of the spectrographs used in this thesis.

Spectrograph	FWHM [$\mathrm{km\,s^{-1}}$]
FIRE	59
GNIRS	136
ISAAC	46
LIRIS	477
NIRI	465
NIRSPEC	122
SINFONI	124
SOFI (MR)	323
SOFI (LR)	535
P200 TRIPLESPEC	88
ARC TRIPLESPEC	97
XSHOOTER	25
SDSS/BOSS	152
UVES	3
HAMBURG-ESO	400

The monochromatic continuum luminosity at 5 μm was also computed by linearly interpolating through the WISE photometric data points. 5 μm luminosities were derived in this way for 434 quasars up to redshift $z = 3.4$. At higher redshifts, the longest wavelength WISE pass-band ($W4$) is at $< 5\mu$m in the quasar rest-frame.

1.6 INSTRUMENTAL BROADENING

Throughout this thesis, reported line-width measures are corrected for instrumental broadening by subtracting the resolution of the spectrograph in quadrature. Because the quasar emission line profiles are typically non-Gaussian, this deconvolution procedure is only approximate. The spectrograph resolutions, which we estimate from the line widths in the observed sky spectra, are given in Table 1.6. The resolutions are generally small relative to the widths of quasar broad emission lines (FWHM $\sim 4000\,\mathrm{km\,s^{-1}}$).